Controlled Crystallization of Calcium Phosphate Apatites

L. M. Rodríguez-Lorenzo and M. Vallet-Regí*

Departamento de Química Inorgánica y Bioinorgánica, Facultad de Farmacia, Universidad Complutense de Madrid, 28040 Madrid, Spain

Received March 8, 2000. Revised Manuscript Received June 5, 2000

The growing necessity of biomaterials has increased the interest in calcium phosphates, particularly apatites. Small differences in stoichiometry, crystallinity, morphology, etc. could contribute to the different clinical behaviors observed, so perfect control of the synthesis parameters and their influence in the characteristics of the samples is a must. In the present work, a crystallization set able to produce massive and reproducible quantities of different calcium phosphates is presented. Apatites with different stoichiometries and morphologies are prepared, and the effects of varying synthesis conditions are analyzed. Temperatures in the range 25−37 °C are necessary to obtain apatites with crystal sizes in the range of adult human bone. Longer reaction times produce increased Ca/P ratios. Aging of the precipitated powder can lead to the incorporation of minor quantities of carbonate. It is possible to force the incorporation of carbonate ions into the apatitic structure without introducing monovalent cations.

Introduction

There is an escalating interest in calcium phosphates, particularly apatites, which seems to be driven mainly by the requirements for the development, understanding, and manufacture of biomaterials.[1]

Traditional clinical applications of calcium phosphates have mainly focused on highly crystalline ceramics. More recently cement-type reactions have been developed to produce low crystalline apatite products. An interesting possibility is the manufacture of poorly crystalline, low particle size apatite powders that are subsequently processed in association with matrices to keep their characteristics and potential.[2] The latter possibilities result in crystal sizes of the products in the range of human tissues[3] (1300 × 300 Å for adult enamel, 200 × 40 Å for dentin, and 250 × 30 Å for bone). Therefore, properties such as bioactivity, dissolution range, resorption, etc. will be close to those of natural bones.

In recent years, the rising interest in synthetic calcium phosphates has produced a huge amount of literature detailing new routes or modifications of old methods to produce calcium phosphates.[1,3−11] Hydroxyapatites ($Ca_{10-x}(HPO_4)_x(PO_4)_{6-x}(OH)_{2-x}$; $0 \le x \le 2$) continue to be the most important among calcium phosphates studied. Whereas previous emphasis has been restricted to controlling the stoichiometry of the products, the aim now is to controlling the morphology as well, as dictated by specific applications.[1]

Among the available methods, those based on precipitation from aqueous solutions are the most suited for preparation of the appreciable quantities of apatites necessary for processing both, into ceramic bodies and in association with different matrixes.

The difficulty with most of the conventional precipitation methods used is the synthesis of well-defined and reproducible orthophosphates.[6,7] Problems can arise because the factors governing the precipitation, pH, temperature, Ca/P ratio of reagents, etc. are not usually precisely controlled and can lead to slightly different products in stoichiometry, crystallinity, morphology, etc. that could contributed to the different "in vivo/in vitro" behavior described.[2,12−15]

The aim of the current work is the development of a methodology able to produce massive and reproducible

* Corresponding author at former address. Present contact information: telephone, 34 91 3941861; fax number, 34 91 3941786; e-mail: vallet@eucmax.sim.ucm.es.

(1) Elliott, J. C. Recent Studies of Apatites and other Calcium Orthophospates. In *Calcium Phosphate Materials, Fundamentals*; Bres E., Hardouin P., Eds.; Sauramps Medical: Monpellier, 1998; p 25.

(2) Rey, C. Calcium Phosphate for Medical Applications. In *Calcium Phosphate in Biological and Industrial Systems*; Amjad, Z., Ed.; Kluwer Academic Publishers: Boston, 1998; p 217.

(3) LeGeros, R. Z. Calcium Phosphates in Oral Biology and Medicine. *Monographs in Oral Science 15*; Karger: Basel, 1991.

(4) Elliott, J. C. Structure and Chemistry of the Apatites and other Calcium Orthophosphates. *Studies in Inorganic Chemistry 18*; Elsevier: Amsterdam, 1994.

(5) de Groot, K. *Bioceramics of Calcium Phosphate*; de Groot, K., Ed.; CRC Press: Boca Raton, 1983; p 100.

(6) Narasaraju, T. S. B.; Phebe, D. E. *J. Mater. Sci.* **1996**, *31*, 1.

(7) Suchanec, W.; Yoshimura, M. *J. Mater. Res.* **1998**, *13*, 98.

(8) Aoki, H. *Medical Applications of Hydroxyapatite*; Ishiyaku Euroamerica, Inc.: Tokio, 1994.

(9) Driessens, F. C. M.; Verbeeck, R. M. H. *Biominerals*; CRC Press: Boca Raton, 1990.

(10) de Groot, K. *Ceram. Int.* **1993**, *19*, 363.

(11) van Raemdock, W.; Ducheine, P.; De Meester, P. Calcium Phosphate Ceramics. In *Metal and Ceramic Biomaterials*; Ducheine, P., Hastings, H., Eds.; CRC: Boca Raton, 1984; Vol. 2.

(12) Uchida, A.; Yamashita, Y.; Sonoda, J.; Yamazaki, T.; Araki, N.; Ueda, T.; Yosikawa, H. *Bioceramics 12*; Ohgushi, H., Hastings, G. W., Yoshikawa, T., Eds.; World Science Publishers: Singapore, 1999; p 11.

(13) Ohura, K.; Matsuda, N.; Hamanishi, C.; Tanaka S. *Bioceramics 12*; Ohgushi, H., Hastings, G. W., Yoshikawa, T., Eds.; World Science Publishers: Singapore, 1999; p 237.

(14) Albrektson, T. In *Handbook of Biomaterials Properties*; Black, J., Hastings, G., Eds.; Chapman & Hall: London, 1998; p 500.

10.1021/cm001033g CCC: $19.00
Published on Web 08/04/2000

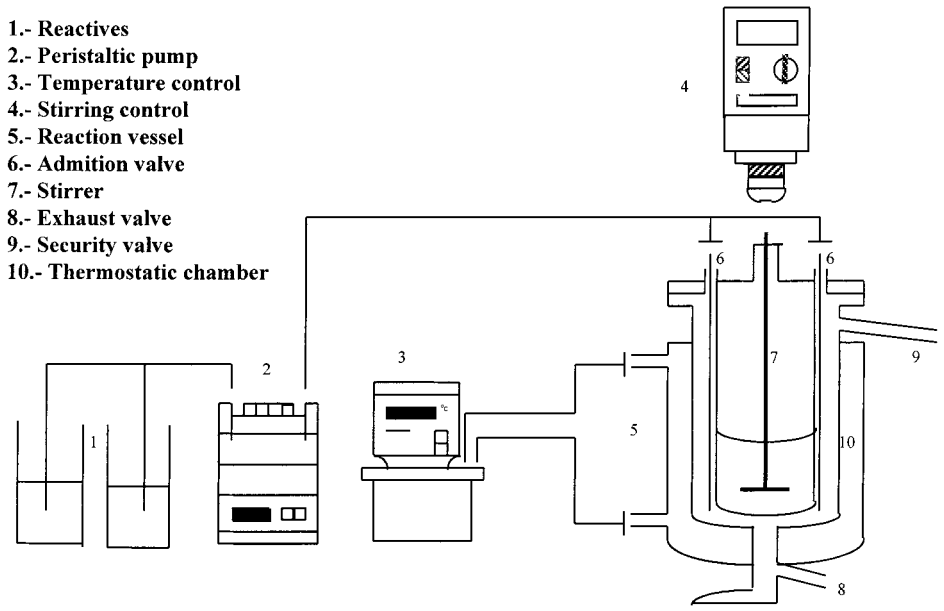

Figure 1. Crystallization set.

quantities of apatite that can be appropriate for any specific application or processing requirements by controlling composition, impurities, morphology, and crystal and particle size.

For quantitative reactions in solution, the reactants must be salts of calcium and phosphates with ions that are unlikely to be incorporated into the apatite lattice. Since it has been claimed that NO_3^- and NH_4^+ are not incorporated into crystalline apatites, or in the case of NH_4^+ present a very limited incorporation,[4] the chosen reaction for the present work was[6,7,16]

$$10Ca(NO_3)_2{\cdot}4H_2O + 6(NH_4)_2HPO_4 + 8NH_4OH \rightarrow Ca_{10}(PO_4)_6(OH)_2 + 20NH_4NO_3 + 6H_2O \quad (1)$$

In the present study, apatites with different stoichiometry and morphology have been prepared and the effects of varying synthesis conditions on stoichiometry, crystallinity, and morphology of the powder are analyzed. The effects of varying concentration of the reagents, the temperature of the reaction, reaction time, initial pH, aging time, and the atmosphere within the reaction vessel were studied.

Experimental Section

Apatite Precipitation. Apatites with different stoichiometries and morphologies have been prepared following eq 1. A crystallization set depicted in Figure 1 has been employed, and the effects of varying synthesis conditions on stoichiometry and morphology of the powder are reported. Reactants shown in eq 1 were dropped simultaneously at a flow rate of 22 mL/min. The obtained powders were washed several times with distilled water and dried at 104 °C. The effects of varying concentration of the reagents (0.001−1 M), the temperature of the reaction (25−90 °C), reaction time (0−24 h), initial pH (7−12), aging time (0−30 days), and the atmosphere within the reaction vessel (N_2, air, CO_2) were studied.

Apatite Characterization. The precipitated hydroxyapatite powders were chemically and physically characterized using atomic absorption spectroscopy, UV−vis spectroscopy, CHN analysis, thermogravimetric analysis, FTIR spectroscopy, X-ray diffraction, scanning and transmission electron microscopy (SEM and TEM respectively), electron diffraction (ED), specific surface area analysis (A), and X-ray fluorescence. Atomic absorption for Ca was performed on a Perkin-Elmer 2280 using acetylene flame and LaO_2 for background correction. Phosphorus was analyzed in a Beckman DU-7 using the molybdenovanadate method. Both measurements were done in the same solution, and Ca/P ratio was calculated from them. The carbonate ions content of the samples was measured by elemental analysis C, H, N in a Perkin-Elmer 2400 CHN analyzer. The detection limit is 0.1%. Thermogravimetric analyses were performed in a Seiko TG/DTA 320 thermobalance. FTIR spectra were recorded in a Nicolet Magna-IR spectrometer from 500 to 4000 cm^{-1} using the KBr technique and operating in the transmittance mode. X-ray diffraction was performed with a Phillips X'Pert diffractometer using Cu Kα radiation at 50 mA, 40 kV. Scans were performed in step mode between 2θ values of 4° and 120° with a step size of 0.2°and 10 s per step. Crystal size has been determined by using Scherrer equation[17] and Rietveld analyses were performed with the Philips PC−Riet software.[18−22] Morphology of particles was studied by SEM in a JEOL 6400 equipped with a Pentafet super ATW system analyzer which allows sample composition to be studied by energy dispersive spectroscopy (EDS). Crystal size and shape was studied by TEM in a JEOL 2000FX microscope where ED patterns were also recorded. Specific surface area was calculated using the BET method[23] from a N_2 adsorption isotherm obtained in a Micromeritics ASAP2010 porosimeter operating between 10 and 127 KPa. Pore volume was calculated from the desorption branch of the isotherm by using the BJH method[24] that relates the amount of adsorbate lost in a desorption step to the average sizes of

(15) Hench, L. L. In *Biomaterials Science*; Ratner, B. D., Hoffman, A. S., Schoen, F. J., Lemons, J. E., Eds.; Academic Press: San Diego, 1996; p 73.
(16) Puajindanetr, S.; Best, S. M.; Bonfield, W. *Br. Ceram. Trans.* **1994**, *93*, 96.
(17) Scherrer, W. N.; Jenkins, R. *Adv. X-ray Anal.* **1983**, *26*, 141.
(18) Rietveld, H. M. *Acta Crystallogr.* **1967**, *22*, 151.
(19) Rietveld, H. M. *J. Appl. Crystallogr.* **1969**, *14*, 65.
(20) Young, R. A. The Rietveld Method. *IUCr Monographs on Crystallography 5*; Oxford University Press: Oxford, 1993.
(21) Young, R. A.; Wiles, D. B. *Adv. X-ray Anal.* **1981**, *24*, 1.
(22) Howard, C. J.; Hill, R. J. AAEC report M112, 1986.
(23) Brunauer, S.; Emmett, P. H.; Teller, E. *J. Am. Chem. Soc.* **1938**, *60*, 309.
(24) Barret, E. P.; Joyner, L. S.; Halenda, P. P. *J. Am. Chem. Soc.* **1951**, *73*, 373.

pores emptied in the step. X-ray fluorescence was performed with a Bruker AXS equipment.

Results and Discussion

Hydroxyapatite is, thermodynamically, the most stable calcium phosphate at the assayed conditions.[25] Each of the products obtained were immediately identified as apatitic products by means of their XRD patterns, independently of other analysis such as the Ca/P ratio or carbonate content. Whatever this means, the direct precipitation of OHAp or the formation of an amorphous phase which immediately is transformed into an apatitic product has not been investigated. But it is worth mentioning that it was not possible to obtain an amorphous phase which is predicted to be the first product formed in conditions of high supersaturation such as the used ones.[26−30]

Influence of Concentration of the Reactants. Chemical analysis, XRD patterns, and IR spectra of samples obtained at different concentrations (rest of conditions identical) show no differences within experimental error. Figure 2 gives an example of XRD patterns of products obtained at different temperatures. Since the aim of the current work is to study the influence of the reaction parameters on the characteristics of the precipitated powder in those reactions which allow appropriate quantities to be obtained to process ceramic bodies or composites that can be useful as biomaterials, and upon checking that concentration does not have a dramatic influence on the characteristic of the product, the study of the influence of the other parameters mentioned will be studied in the higher concentration assayed.

Influence of the Temperature of Reaction. Figure 2 shows the XRD pattern of samples synthesized at different temperatures. It is clearly observed that the higher the temperature, the lower the maximum width, indicating that a bigger coherent diffraction domain is obtained at higher temperatures. When this domain is calculated by using the Scherrer equation, values from 100 Å at 25 °C to 200 Å at 90 °C are obtained from the 300 peak and from 200 Å at 25 °C to 800 Å at 90 °C when the 002 peak is considered. The increase in the value calculated from 002 peak was greater than that calculated from the 300 peak reflecting a higher acicular shape of the crystals obtained at higher temperatures. It is noticeable that the crystal sizes of the samples synthesized at 25 °C are in the range of human bone or dentin while crystal sizes of the sample synthesized at 90 °C are in the range of dental enamel.[3]

Figure 3 indicates that the specific surface area decreases as the temperature of reaction is increased. Since specific surface area is related to particle size, it is possible to amend that this parameter has not only influence on the crystal size and shape but also on particle size.

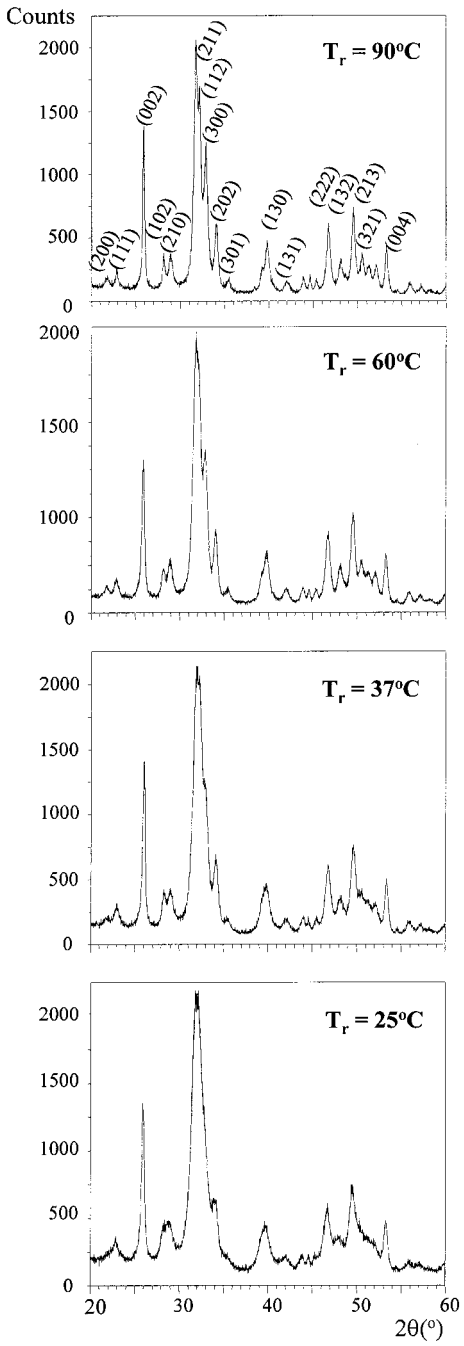

Figure 2. XRD patterns of apatites synthesized at different temperatures. Other conditions are identical.

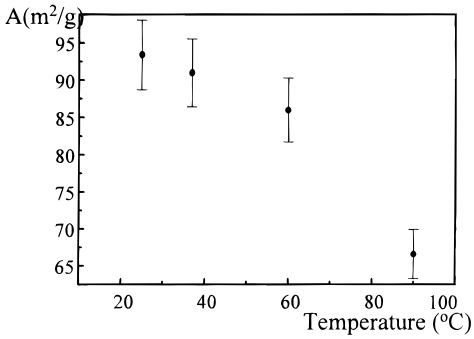

Figure 3. Specific surface area for apatites obtained at different temperatures.

Influence of Reaction Time. Figure 4 shows that longer reaction times yield apatites with higher Ca/P

(25) Rodríguez Lorenzo, L. M. Síntesis, procesado y propiedades de cerámicas de fosfato de calcio con interés clínico. Tesis Doctoral, Universidad Complutense de Madrid 1999.
(26) Lazic, S. *J. Cryst. Growth* **1995**, *147*, 147.
(27) Abbona, F.; Lundager-Madsen, H. E.; Boistelle, R. *J. Cryst. Growth* **1986**, *74*, 581.
(28) Tung, M. S.; Brown, W. E. *Calcif. Tissue Int.* **1983**, *35*, 783.
(29) Betts, F.; Blumenthal, N.; Posner, A. S. *J. Cryst. Growth* **1981**, *53*, 63.
(30) Nancollas, G. H.; Tomazic, B. *J. Phys. Chem.* **1974**, *78*, 2218.

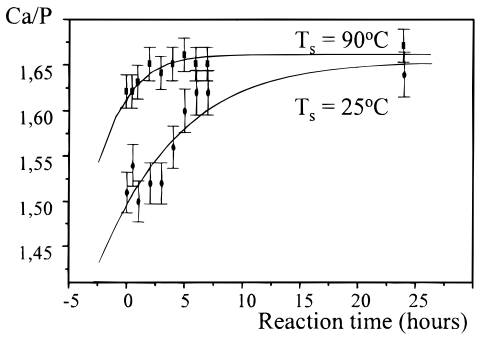

Figure 4. Evolution of Ca/P ratio with reaction time for apatites synthesized at 25 °C and 90 °C.

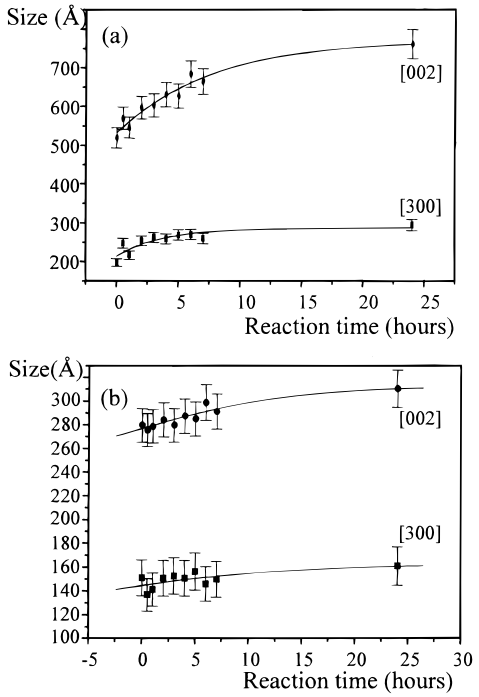

Figure 5. Evolution of crystal size obtained from the Scherrer equation from the peaks [300] and [002] for apatites obtained at (a) 90 °C and (b) 25 °C.

ratios, resulting in a decrease of the calcium deficiency of the sample. When the reactions are carried out at 90 °C, 2 h are necessary to obtain a product with a Ca/P ratio of 1.67, i.e., OHAp, while shorter times and/or lower temperatures yield calcium deficient apatite, i.e., $Ca_{10-x}(HPO_4)_x(PO_4)_{6-x}(OH)_{2-x}$; $0 \le x \le 2$ (Ca/P < 1.67).

Figure 5 depicts the crystal size evolution. Crystal size is higher as a result of higher times of reaction. Again a higher increase of the value calculated from 002 peak than of the value calculated from 300 peak is observed. The evolution of crystal shape and size can be observed in the micrograph shown on Figure 6. Crystals of average size 220 Å were obtained at 25 °C and at the so-called time of reaction zero, and crystals around 900 Å are observed at 90 °C and 24 h of reaction. ED patterns reflect the differences in crystal sizes. While ED pattern of powders obtained at short times of reaction are characteristic of polycrystalline materials, ED patterns of the product with longest time of reaction and temperature indicate a well crystallized material. Both patterns are compatible with the OHAp structure.

Table 1 shows specific surface areas of hydroxyapatites synthesised at different reaction times at 25 and 90 °C. An increase of particle size can be deduced for the highest reaction time at both 25 and 90 °C. Table 1 also shows the values obtained for pore volume and pore diameter. The volume occupied by pores remains in the same range, indicating no dependence on reaction time or temperature. The diameter of the pores is higher for samples with lower surface area, indicating that at higher temperatures bigger particles with bigger pores are obtained. So an increase in the reaction time will affect not only stoichiometry, but also crystal size and shape and particle size.

Table 1. Specific Surface Area, Pore Volume, and Pore Diameter (Obtained from the BJH Method)

T_s[a] (°C)	t_r[b] (h)	A (m^2/g)	V_{BJH} (cm^3/g)	D_{pore} (nm)
25	0	93.4	0.35	11.1
	0.5	99.9	0.41	13.3
	1	100.5	0.42	13.2
	2	100.2	0.40	12.1
	3	89.8	0.39	13.6
	4	95.9	0.38	12.6
	6	88.5	0.33	11.6
	7	96.5	0.31	9.5
	24	78.4	0.32	9.4
90	0	66.6	0.34	17.9
	0.5	56.0	0.40	25.7
	1	59.6	0.35	21.1
	2	55.0	0.28	21.4
	3	59.7	0.38	23.1
	4	53.0	0.35	22.2
	5	56.0	0.40	25.7
	6	51	0.36	24.4
	7	56.6	0.40	25.3
	24	42.1	0.28	24.3

[a] Temperature of synthesis. [b] Reaction time.

Table 2. Ca/P Ratio Calculated from the Rietveld Method and Chemical Analysis and Crystal Size Calculated from the Sherrer Equation

pH	t_r[a] (h)	Ca/P (Rietveld)	Ca/P (AA/UV)	[002] (Å)
7.4	1	1.51	1.50 (5)	290
	7	1.63	1.60 (5)	490
10	1	1.56	1.56 (5)	327
	7	1.65	1.64 (6)	512

[a] Reaction time.

Impurity levels of different apatites were analyzed by X-ray fluorescence to check the adequacy of these powders to manufacturing biomedical devices. Obtained values were as follows As < 1 ppm, Cd < 2 ppm, Hg < 1 ppm, Pb < 10 ppm, and total heavy metals 29 ppm and are acceptable for the production of surgical devices according to ASTM F1185-88 standard.

Influence of pH of Solution. All of the former reactions were studied at pH 10. Owing to recrystallization of $(NH_4)_2HPO_4$ it was impossible to conduct experiments at pH > 10. Experiments developed at an initial pH 7 or 8 result in final pH lower than 4. As a consequence, the obtained powder was not identified as apatite but as dicalcium phosphate, either brushite, monetite, or a mixture of both phases depending on other parameters such as temperature. Thus, a modification in the procedure had to be done in order to study the influence of pH. A diammonium/monoammonium phosphate buffer of pH 7.4 was prepared keeping the Ca/P ratio of reagents. Table 2 shows the Ca/P ratio of the apatite product obtained at different reaction times. (The Ca/P ratio was analyzed by different techniques,

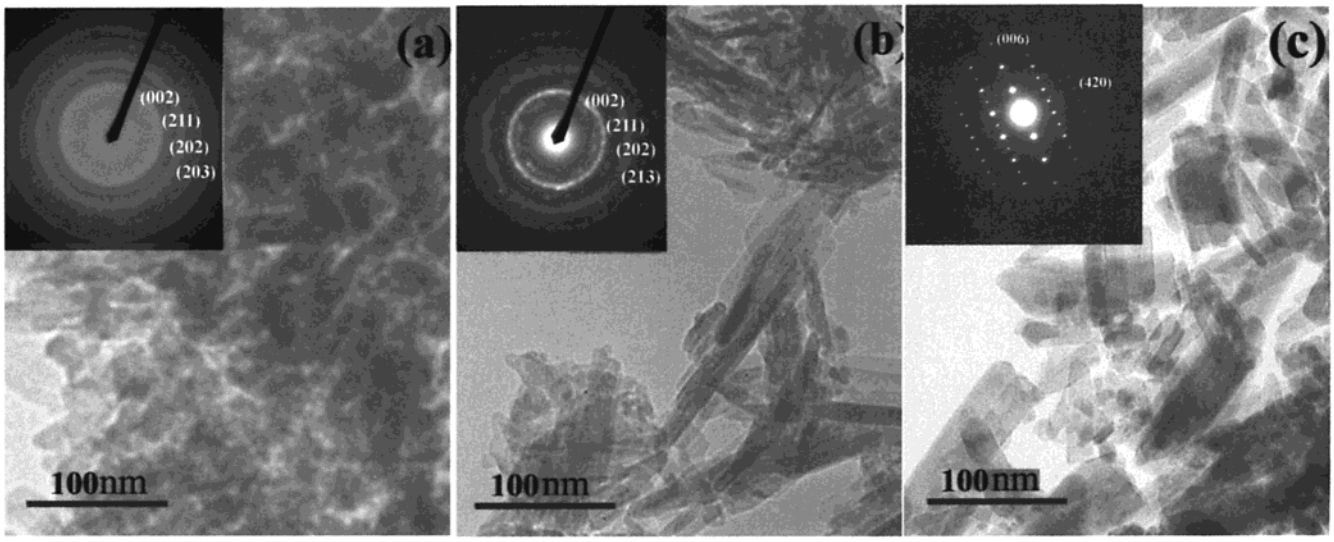

Figure 6. TEM micrographs and ED patterns (inset) of samples obtained at (a) $T_s = 25$ °C, $t_r = 0$ h; (b) $T_s = 90$ °C, $t_r = 0$ h; (c) $T_s = 90$ °C, $t_r = 24$ h.

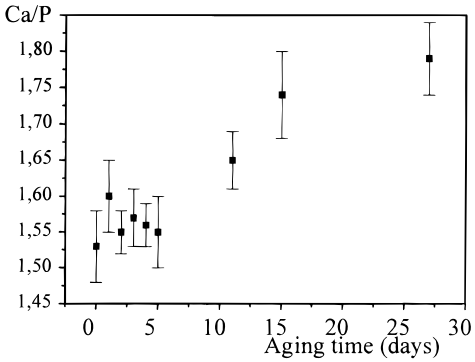

Figure 7. Ca/P ratio of apatites as a function of aging time.

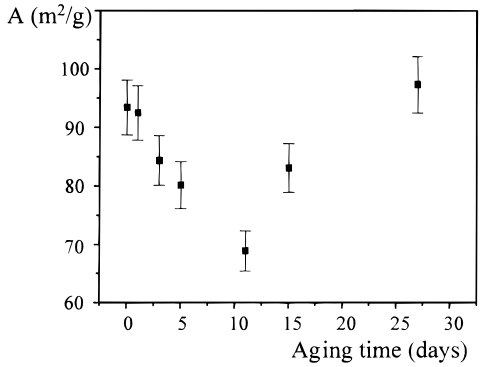

Figure 8. Specific surface area of apatites as a function of aging time.

chemical analysis, and a multiphase Rietveld refinement described elsewhere to ensure the reliability of the results.[31]) An increase in the Ca/P ratio is observed with the time of reaction regardless of the pH studied. In addition, when the same reaction times are compared, it is possible to notice a lower value of Ca/P ratio for the lower pH assayed. The crystal size is also lower at a lower pH as seen in Table 2.

Aging Time. Extensive aging at room temperature of samples synthesized at short reaction times leads to an increase on their Ca/P ratios after 11 days, Figure 7. After 15 days, the Ca/P ratio is higher than 1.67. Also a decrease of surface area can be observed over a time period of 11 days (period in which Ca/P ratio remains below 1.67), followed by a subsequent increase, Figure 8. Two types of phenomena can be considered for explanation. The first one is a rearrangement of grains due to the solubility differences between differently sized grains, resulting in bigger grains growing at the expense of smaller ones and the second one is the solubility of the material. The first effect should predominate during the first 11 days and the second one at latter times. The coincidence of the beginning of the increase of the surface area value with a significant increase of the Ca/P ratio can be correlated with the uptake of carbonate from the medium. It is well-known that a higher carbonate content promotes an increase in solubility.[3,4,32−34] So the preeminence of the solubility can lead to a decrease in particle size reflected in the higher surface area. The IR spectra of the products obtained after 15 days of aging show bands that can be attributed to CO_3^{2-} groups confirming that some carbonate has entered the structure.[32,35−38] The location of CO_3^{2-} groups on the phosphate site explains values of Ca/P ratio higher than 1.67.

Influence of the Atmosphere. Figure 9 depicts the IR spectra of samples synthesized in the same conditions but under different atmospheres. A NO_3^- band and CO_3^{2-} bands can be observed in samples obtained in N_2 and CO_2 atmosphere, respectively. Carbonate band positions indicate that these groups are mainly located in phosphate positions. X-ray analysis shows a decrease in the crystallinity of the materials when the sample has been synthesized in CO_2 as a consequence of the

(31) Vallet-Regí, M.; Rodríguez-Lorenzo, L. M.; Salinas, A. J. *Solid State Ionics* **1997**, *101−103*, 1279.

(32) Rey, C.; Collins, B.; Goehl, T.; Dickson, I. R.,; Glimcher, M. J. *Calcif. Tissue Int.* **1989**, *45*, 157.

(33) Michel, V.; Ildefonse, P.; Morin, G. *Appl. Geochem.* **1995**, *10*, 145.

(34) Okazaki, M.; Moriwaki, Y.; Aoba, T.; Doi, Y.; Fakahashi, J. *Caries Res.* **1981**, *15*, 477.

(35) Nelson, D. G. A. *J. Dental Res.* **1981**, *60*, 1621.

(36) LeGeros, R. Z.; Tung, M. S. *Caries Res.* **1983**, *17*, 419.

(37) LeGeros, R. Z. *Nature* **1965**, *206*, 403.

(38) Rey, C.; Renugopalakrishnan, V.; Collins, B.; Glimcher, M. J. *Calcif. Tissue Int.* **1991**, *49*, 251.

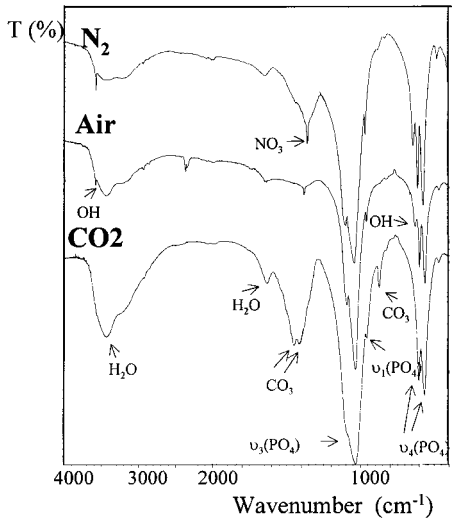

Figure 9. IR spectra of apatites synthesised under different atmospheres.

incorporation of these groups. X-ray fluorescence shows no presence of impurity ions such as Na^+ or K^+. It is possible to conclude that a CO_2 atmosphere leads to the formation of carbonate apatite in which for every negative charge lost when a CO_3^{2-} replaced a PO_4^{3-}, another negative charge is lost by the loss of an OH^- ion; the loss of these two negative charges is then compensated by the loss of two positive charges through the formation of a calcium site vacancy and so on without the introduction of impurity ions, i.e., Na^+, K^+. The percentage of carbonate measured by elemental analysis was 4.7%. On the other hand, when a N_2 atmosphere is used, some nitrate is detected in the IR spectrum and the presence of nitrogen is then confirmed by elemental analysis (C = 0.06; N = 1.01). The nitrate comes probably from the calcium nitrate reagent used in the synthesis reaction and not completely eliminated in the washing step, as happened in the others atmospheres assayed. Therefore, this kind of atmosphere, frequently used for the synthesis of OHAp, can avoid the minor uptake of CO_3^{2-} but can introduce a different contamination which convenience should be evaluated in each particular synthesis.

Concluding Remarks

A crystallization set able to produce massive and reproducible quantities of different calcium phosphates has been installed. The synthesized apatites fulfill the normative ASTM F1185-88 that enables these powders to be used for the development of surgical implants.

The main results of the studied variations in the reaction conditions are, higher concentrations of reagents produce higher amounts of products with minor differences in their characteristics, allowing the production of homogeneous sets of materials. Temperatures in the range 25−37 °C are necessary to obtain apatites with crystal size in the range of adult human bone or dentin while 90 °C are necessary to obtain apatites with crystal sizes in the range of enamel. Higher reaction times lead to apatites with higher Ca/P ratios. Aging of the precipitates can lead to the incorporation of minor quantities of carbonate. Atmosphere of N_2 or CO_2 can force the incorporation of impurity ions into the apatitic structure.

It is possible to control stoichiometry, crystallinity, and morphology of calcium phosphate apatites as a function of reaction conditions.

Acknowledgment. This work was supported by CICYT (Spain) through research project MAT99-0466.

CM001033G